Arabian Journal of Chemistry (2016) 9, S1464–S1477

King Saud University

Arabian Journal of Chemistry

www.ksu.edu.sa
www.sciencedirect.com

ORIGINAL ARTICLE

Equilibrium, kinetics and thermodynamic parameters for adsorptive removal of dye Basic Blue 9 by ground nut shells and Eichhornia

Sumanjit *, Seema Rani, R.K. Mahajan

Department of Chemistry, Guru Nanak Dev University, Amritsar 143005, India

Received 16 September 2011; accepted 17 March 2012
Available online 28 March 2012

KEYWORDS

Adsorption;
Basic Blue 9;
Adsorbents;
Kinetics;
Isotherm

Abstract Adsorption of dye Basic Blue 9 (BB9) was studied using ground nut shells charcoal (GNC), and Eichhornia charcoal (EC) as adsorbents. The characterization was done with FTIR spectroscopy, scanning electron microscopy and X-ray diffraction. Batch adsorption studies have been investigated by measuring the effect of pH, adsorbent dose, adsorbate concentration, contact time, temperature, and ionic strength. Adsorption of the dye increased with increase in contact time, temperature, amount of adsorbent and initial concentration. The kinetic experimental data were fitted to pseudo-first order, pseudo-second order, intra-particle diffusion, Elovich model and Bangham's model and corresponding constants were calculated and discussed. Pseudo-second order kinetics was found to describe the adsorption of dye BB9 on both the adsorbents and rate is mainly controlled by intra particle diffusion. A study of five isotherm models; Langmuir, Freundlich, Temkin, Dubinin and Radushkevich and generalized isotherms have been made and important thermodynamic parameters have been obtained. The adsorption of BB9 onto GNC and EC was spontaneous and endothermic as concluded from thermodynamic assays. Experimental results confirmed that dye BB9 can be successfully removed from the aqueous solutions economically and efficiently.

1. Introduction

Synthetic dyes are widely used in the industries such as textile, leather, paper, plastic, to color their final products (Chiou and Li, 2002). Wastewater from fabric dyeing industry is a considerable source of environmental contamination. The effluent from the dyeing and finishing processes is characterized by a low biodegradability (Barka et al., 2010). Color is the first contaminant to be recognized in waste water and the presence of very small amount of dye in water is highly visible and undesirable (Crini, 2008). Dyes have been found to be stable to light

* Corresponding author. Tel.: +91 183 2256818; fax: +91 183 2258820.
E-mail address: sumangndu@yahoo.co.in (Sumanjit).
Peer review under responsibility of King Saud University.

ELSEVIER Production and hosting by Elsevier

http://dx.doi.org/10.1016/j.arabjc.2012.03.013
1878-5352

Nomenclature

a,b	Elovich constants.	K_L	constant of Langmuir isotherm, L mg^{-1}.
C_o	initial concentration (mg/L).	K_T	constant of Temkin isotherm, L mg^{-1}.
C_e	equilibrium concentration (mg/L).	m	mass of adsorbent per liter of solution, gL^{-1}.
C_m	maximum adsorption capacity of adsorbent, mg g^{-1}.	q_e	amount of dye adsorbed at equilibrium (mg/g).
k_{id}	intraparticle diffusion rate coefficient.	q_t	amount of dye adsorbed at time t (mg/g).
k_f	rate coefficient of pseudo first order adsorption model, min^{-1}.	R	Universal gas constant, 8.314 J $mol^{-1}K^{-1}$.
k_o	coefficient in Bangham's equation.	R^2	correlation coefficients.
k_s	rate coefficient of pseudo second order adsorption model, gm/(mg min).	R_L	separation factor, dimensionless Hall constant.
K_F	constant of Freundlich isotherm $(mg/g)(L/mg)^{1/n}$.	t	time (min).
K_G	constant of generalized isotherm, L mg^{-1}.	ΔG	Gibb's free energy of adsorption, kJ mol^{-1}.
		ΔH	enthalpy of adsorption, kJ mol^{-1}.
		ΔS	entropy of adsorption, JK^{-1} mol^{-1}.
		α	Bangham's coefficient (< 1).

and oxidizing agent (Unuabonah et al., 2008). Moreover the waste dyes and color released in the effluents interfere with the transmission of light in water bodies, this in turn inhibit the photosynthetic activity of aquatic biota besides direct toxic effects on biota (Lakshmi et al., 2009). Some dyes or their metabolites have toxic as well carcinogenic, mutagenic and teratogenic effect on aquatic life and humans (Gong et al., 2007). Basic Blue 9 (BB9) is an important basic dye widely used for printing calico, dyeing, printing cotton and tannin, and it is used as an antiseptic and for other medicinal purposes (Gupta et al., 2004). The dye BB9 can cause eye burns, which may be responsible for permanent injury to the eyes of human and animals, irritation to gastrointestinal tract with symptoms of nausea, vomiting and diarrhea and also cause methemoglobinemia, cyanosis, convulsion, tachycardia and dyspnea. Contact of BB9 with skin causes irritation (Wang et al., 2008).

In order to remove dyes from aqueous solutions many chemical or biological treatments have been used either individually or together (Alpat et al., 2008). Various methods of dye/color removal, including aerobic and anaerobic microbial degradation, coagulation, chemical oxidation, membrane separation, electrochemical treatment, filtration, flocculation, softening, hydrogen peroxide catalysis and reverse osmosis have been proposed from time to time (Coro and Laha, 2001; Mohan et al., 2002; Salem and El-maazawi, 2000; Stephenson and Sheldon, 1996). All these techniques were found inefficient and incompetent because of the stability of the dye toward light, oxidizing agents and aerobic digestion. Dyes also show fairly high solubility in the aqueous media thus it is difficult to remove with the above-mentioned methods for the wastewater treatments. On the basis of comprehensive investigations the adsorption technique was successfully applied and was found to be most appropriate and efficient one (Mittal et al., 2008; Ruthven, 1984). Most conventional adsorption plants use activated carbon, which is an expensive material (Dizge et al., 2008). Investigators have evaluated the feasibility of using low cost substances, such as bottom ash (Leechart et al., 2009), chitosan (Wong et al., 2004), dairy sludge (Sumanjit and Walia, 2008a), sawdust (Sumanjit et al., 2008b), peat (Sun and Yang, 2003), orange peel (Annadurai et al., 2002), banana pith (Namasivayam et al., 1998), rice husk (Sumanjit and Prasad, 2001), bamboo (Chan et al., 2008), perlite (Dogen and Alkan, 2003) etc. as adsorbents for the removal of dyes from wastewater.

The present study investigates the adsorption of BB9 on inexpensive adsorbents namely groundnut shells charcoal (GNC), and Eichhornia charcoal (EC) which are available in plenty in India. The effects of factors such as pH, adsorbent dose, initial concentration, contact time, temperature and ionic strength reported. The kinetics and thermodynamics were analyzed by fitting the data to various kinetics models and isotherm equations.

2. Experimental

2.1. Preparation of adsorbents

Adsorbents ground nut shells and Eichhornia were collected respectively from the local shop and from a pond located in Amritsar, India. The materials were washed with tap water and finally with double distilled water to remove the suspended impurities, dust and soil and then dried in oven. Charcoal was prepared in a very economical way by just burning the material in the absence of free excess of air. Charcoal was sieved through sieves having mesh size 240–200, to remove coarse particles, and the corresponding particle size of 70–75 μ was obtained for both GNC and EC (Lachman and Lieberman, 2009).

2.2. Dye solution preparation

The basic dye, BB9 (Fig. 1) was obtained from S.D fine Chemical, Mumbai, India. An accurately weighed quantity of dye was dissolved in double distilled water to prepare the stock solution (14 mg/L). Experimental solutions of desired concentration were obtained by successive dilutions with double distilled water.

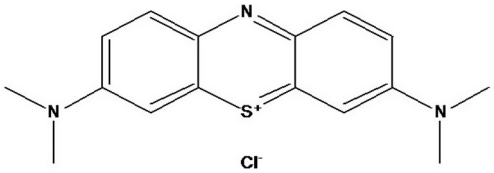

3,7-bis(Dimethylamino)-phenothiazin-5-ium chloride

Figure 1 Structure of Basic Blue 9 (BB9).

2.3. Batch model adsorption studies

Batch adsorption experiments were carried out by shaking 0.1 g of the adsorbent with 100 mL of dye solution of desired concentration in different glass bottles using Metrex water bath shaker. After agitation, samples were withdrawn from the shaker and dye solutions were separated from the adsorbent using Whatman filter paper No. 42. Dye concentration in the supernatant solutions was estimated by measuring absorbance at maximum wavelength (665 nm) of dye with UV–Visible spectrophotometer (1800, Shimadzu, Japan) and computing from calibration curve. The calibration curve is drawn by making serial dilutions and then plotting the absorbance at a wavelength maximum against concentration. The amount of dye adsorbed by the adsorbent was calculated using the following equation.

$$\%\,\text{Removal of dye} = \frac{\text{Co} - \text{Ce}}{\text{Co}} \times 100$$

where Co and Ce (mg/L) are the initial and equilibrium concentrations of the dye respectively.

3. Results and discussion

3.1. FTIR spectroscopy studies

FTIR analysis Fig. 2(a,b) shows the spectrophotometric observations of the dye BB9 and the adsorbents (GNC, EC) in the

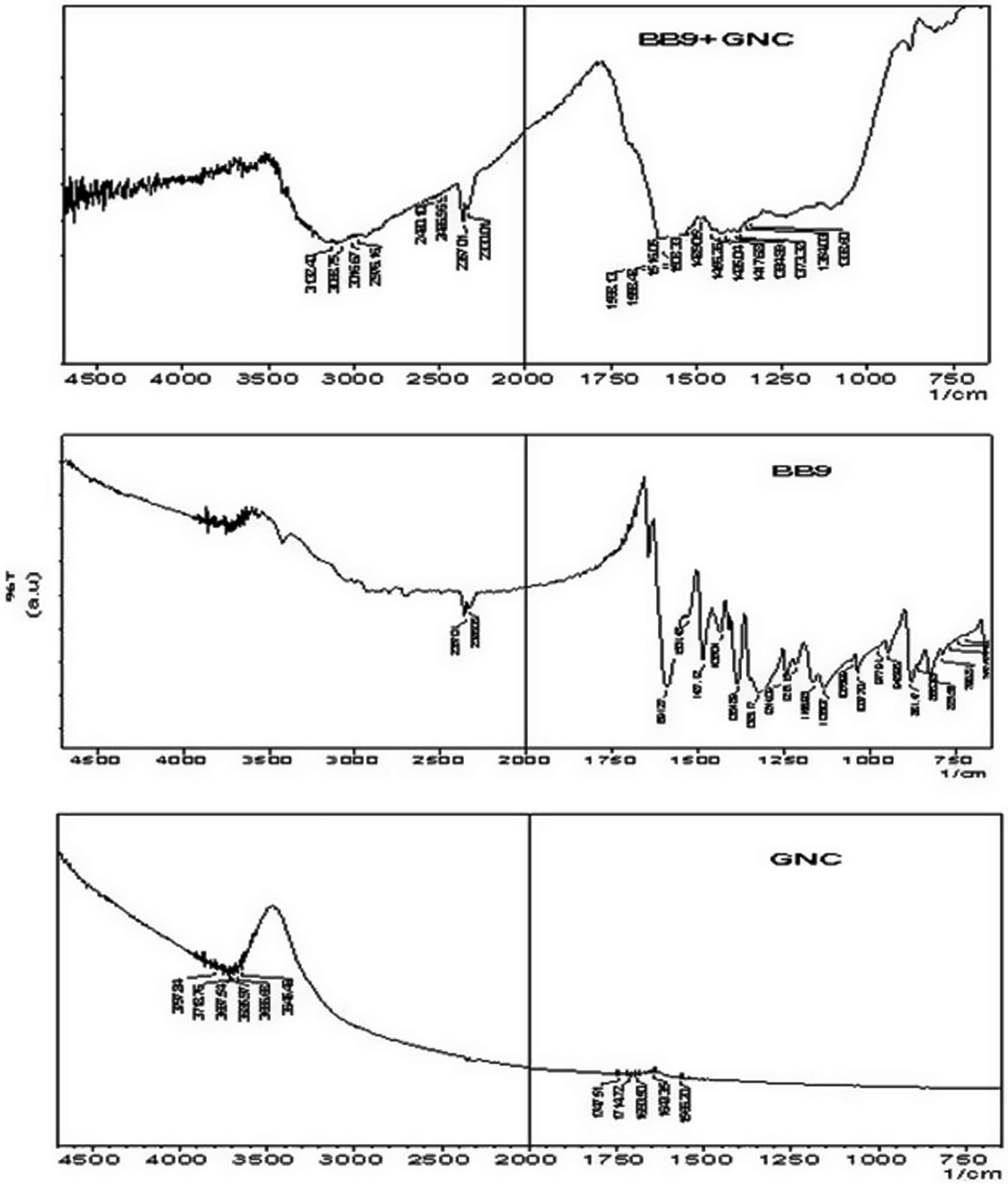

Figure 2 (a) FTIR spectra of GNC, BB9 and dye loaded GNC. (b) FTIR spectra of EC, BB9 and dye loaded EC.

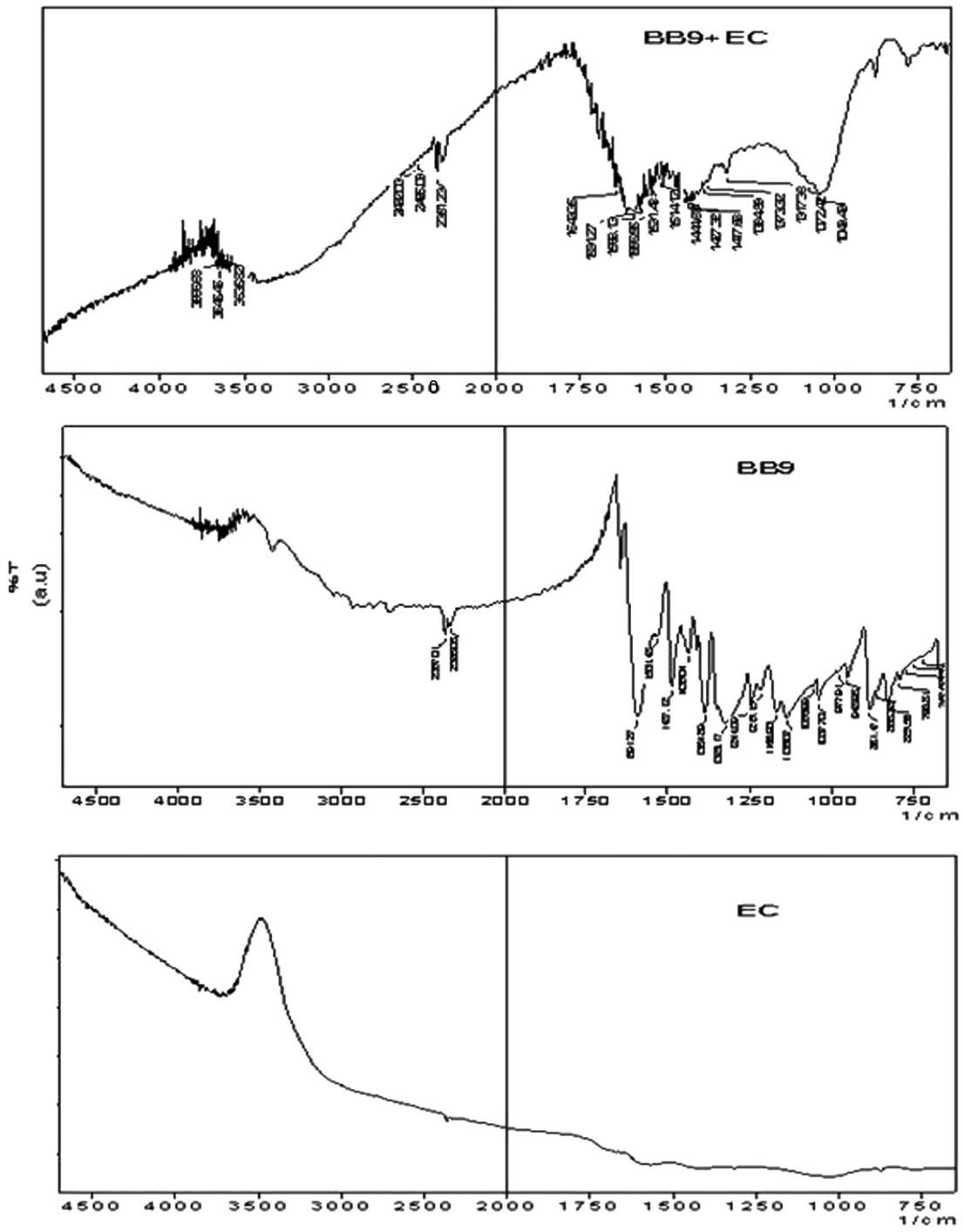

Fig. 2 (*continued*)

range of 400–4000 cm^{-1}. Dye BB9 has sharp peaks at 1136 and 1244 cm^{-1} which can be assigned to C═S and C–N bonds respectively. However a sharp absorption band at 1591 and 2357 cm^{-1} is due to C═N and tertiary amine, respectively.

FTIR spectra of adsorbents giving the broad band of OH stretching vibrations at 3100–3700 cm^{-1} comprise both free and hydrogen bonded hydroxyl groups. On adsorption of the dye by adsorbent, the intensity of sharp peaks corresponding to C═N decreases and shifted from 1591 to 1516 cm^{-1} and intensity of the peak decreases for the bond C═S. In EC the band at 1252 cm^{-1} indicates the presence of carboxylic group. FTIR spectra of BB9 + GNC and BB9 + EC show that peaks in the low frequency region (< 1000 cm^{-1}) which are present in the dye alone are not observed in the dye loaded adsorbents because of the adsorption of dye BB9 on the adsorbent surface. Decreased intensity of sharp peaks concluded that the dye has been functionalized by both the adsorbents.

3.2. X-ray diffraction studies

X-ray diffraction (XRD) technique is a powerful technique to analyze the crystalline and amorphous nature of the material

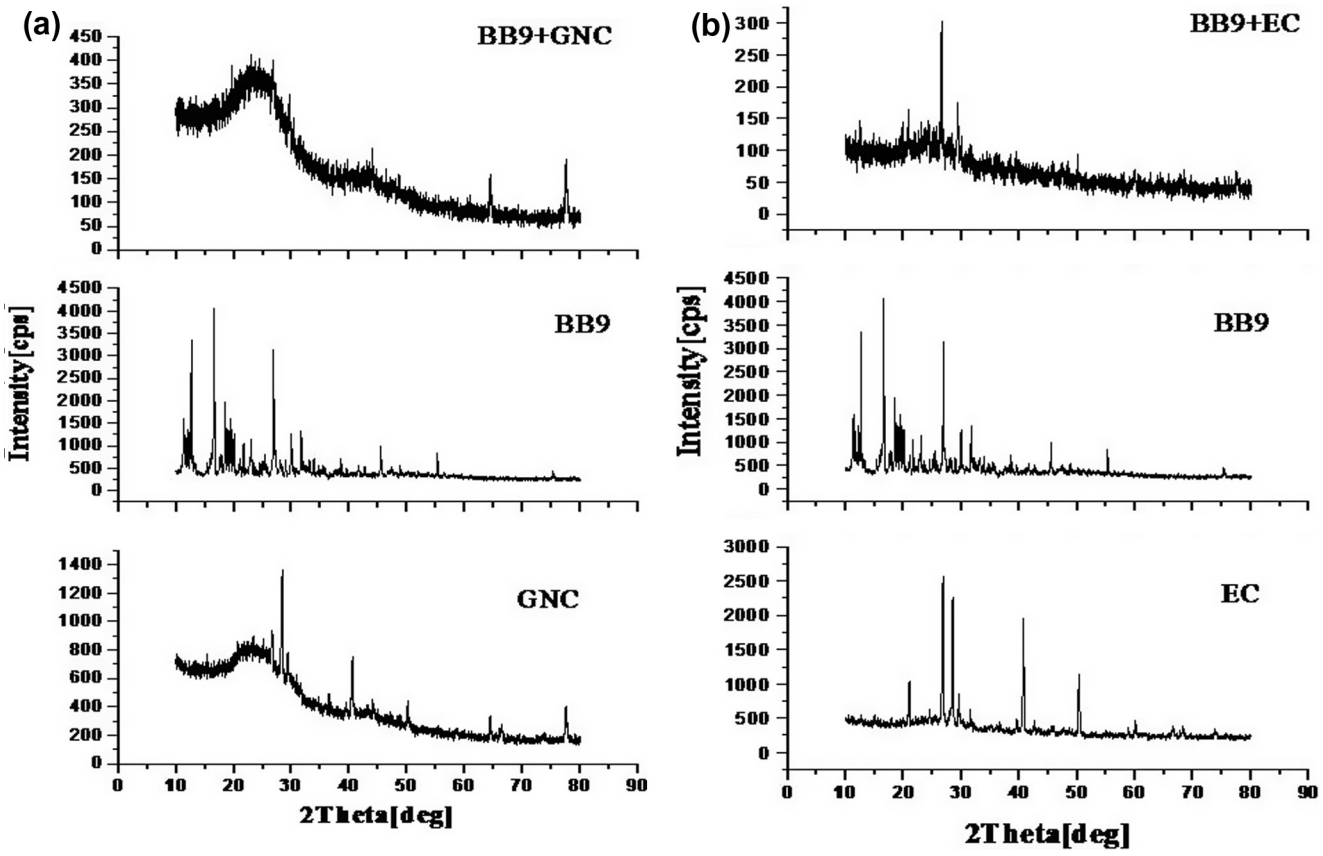

Figure 3 (a) XRD spectra of GNC, BB9 and dye loaded GNC. (b) XRD spectra of EC, BB9 and dye loaded EC.

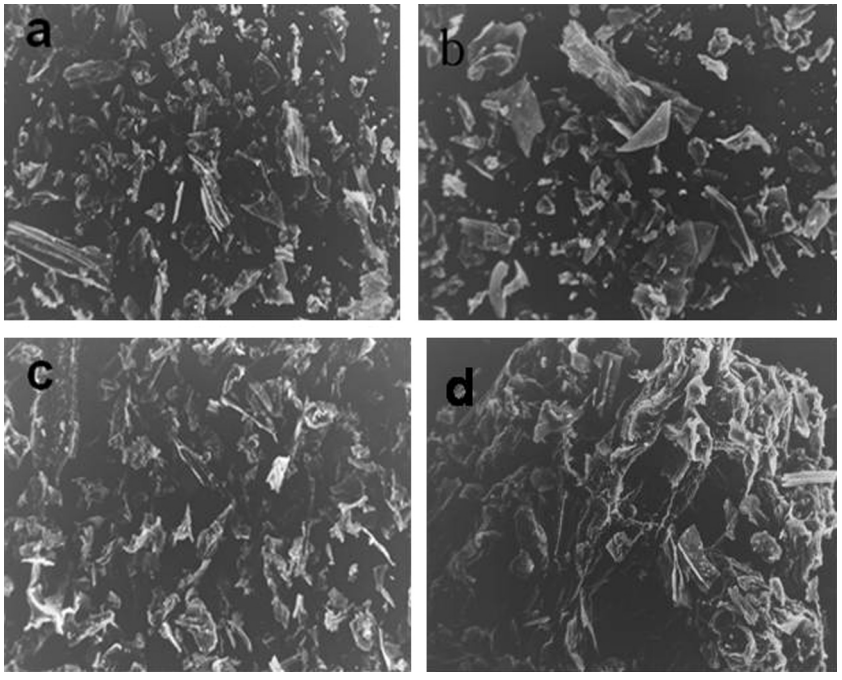

Figure 4 Scanning electron microscope (SEM) images (a) Ground nut shells charcoal (GNC) (b) dye adsorbed GNC (c) Eichhornia charcoal (EC) and (d) dye adsorbed EC.

under investigation. In crystalline material, well defined peaks are observed whereas in non crystalline or amorphous material shows broad peaks instead of sharp peaks. Fig. 3(a,b) shows that well defined peaks are observed in the adsorbent EC as

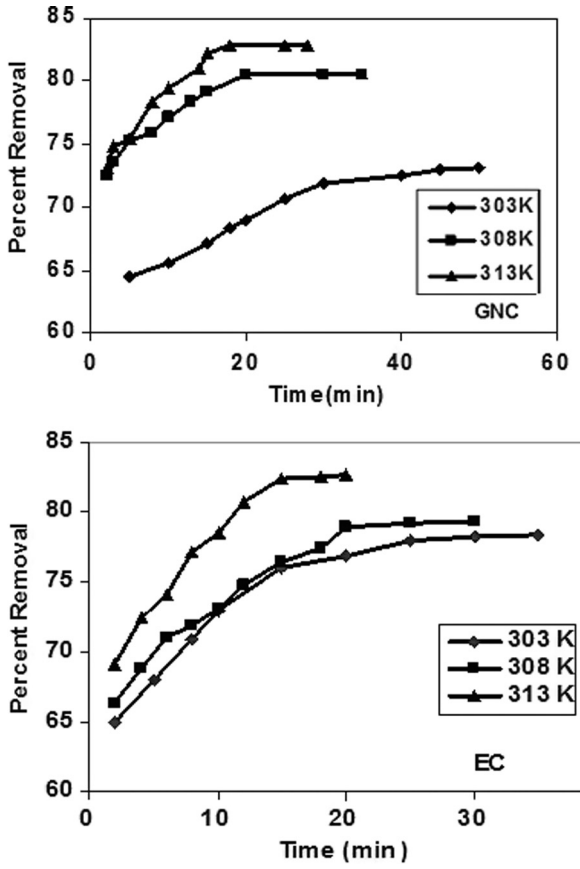

Figure 5 Effect of contact time on the adsorption of BB9 on GNC and EC (Co = 14 mg/L).

compared to GNC which indicates that EC is more crystalline as compared to GNC. When the adsorbent gets loaded by the dye molecules the crystalline nature of the dye was changed into amorphous nature. It has been concluded that the dye molecules diffused into the micro and macro pores of the adsorbent molecules. XRD studies show change in crystallinity of the adsorbent due to adsorption.

3.3. Scanning electronic micrograph studies (SEM)

SEM is widely used to study the morphological feature and surface characteristics of the adsorbent material. In the present study, SEM images of adsorbent before and after adsorption of dye BB9 reveal the porosity and surface texture. In Fig. 4, the surface of dye-loaded adsorbents shows that the surface of GNC and EC is covered with dye molecules.

3.4. Effect of contact time

The equilibrium time is the time needed when maximum adsorption takes place. Fig. 5 shows the effect of contact time on the adsorption of dye BB9 onto GNC and EC at different temperatures. The nature of adsorption process will depend on the physical and chemical characteristics of the adsorbents and also on the system conditions. The amount of dye adsorbed increases with increase in contact time. The contact time curve shows rapid adsorption of BB9 in first 15 min by both the adsorbents followed by the gradual increase of adsorption rate

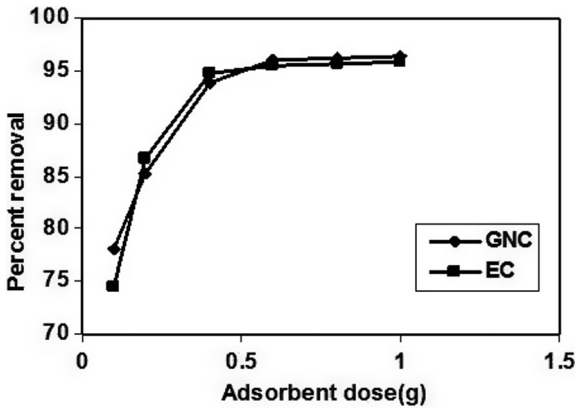

Figure 6 Effect of adsorbent dose on percentage dye removal (Co = 14 mg/L).

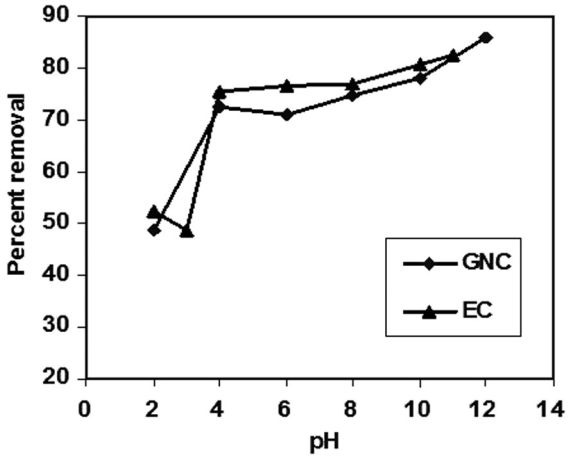

Figure 7 Effect of pH on adsorption of dye BB9 on GNC and EC (Co = 14 mg/L adsorbent dosage = 1 g/L).

and ultimately reaches saturation. The initial rapid phase may be due to increased number of available vacant sites of the adsorbent at the initial stage. The equilibrium time for EC is 30, 25, 15 min and for GNC 45, 20, 18 min at 303, 308 and 313 K, respectively.

3.5. Effect of adsorbent dose

Fig. 6 shows the effect of adsorbent dose on the percentage removal of BB9 by GNC and EC as adsorbents. With increase in the adsorbent dose of GNC and EC from 0.1 to 1.0 g the percentage removal increases up to 96.4% and 95.8% respectively. A large mass of the adsorbent could adsorb large amount of dye due to the availability of more adsorption sites and more surface area of adsorbent.

3.6. Effect of temperature

Temperature is an important factor for the adsorption process. To examine the effect of temperature, an adsorption study of BB9 was performed at three different temperatures, and is illustrated in Fig. 5. It has been believed that temperature generally has two major effects on the adsorption process.

Increasing the temperature will increase the rate of diffusion of the adsorbate molecule across the external boundary layer and in the internal pores of the adsorbent particles. In addition, changing the temperature will change the equilibrium capacity of particular adsorbate (Wang and Li, 2007). Normally adsorption is exothermic in nature, so it was expected that with increase in temperature, adsorption capacity of adsorbents must be decreased. However if adsorption process is controlled by diffusion process (intra-particle transport diffusion), the sorption capacity will increases with increase in temperature due to endothermicity of diffusion process. An increase in temperature results in an increased mobility of the adsorbate and a decrease in the retarding forces acting on the diffusing adsorbate. Increase in adsorption capacity with increase in temperature may be partly attributed to the chemisorptions (Lakshmi et al., 2009).

3.7. *Effect of pH*

The pH of the solution affects the surface charge of the adsorbents as well as the degree of ionization of the materials present in the solution. The hydrogen ions and hydroxyl ions are adsorbed quite strongly, and therefore, the adsorption of other ions is affected by the pH of the solution. The change of pH affects the adsorptive process through the dissociation of functional groups on the active site of the adsorbent. This subsequently leads to the shift in reaction kinetics and equilibrium characteristics of the adsorption process .It is a common observation that the surface adsorbs anion favorably at lower pH due to the presence of H^+ ions, whereas, the surface is active for the adsorption of cations at higher pH due to the deposition of OH^- ions (Mall et al., 2005).

Fig. 7 shows the influence of pH on the adsorption capacity of the adsorbents for the removal of BB9. The pH range of the solution considered for this investigation was 2 to 12. The variation of adsorption with pH can be explained by considering the difference in the structures of dyes, as well as nature of the adsorbent. At lower pH the surface has high positive charge density, and under these conditions the uptake of positively charged BB9 would be low due to electrostatic repulsion. With increasing pH, the negative charge density on the surface of adsorbent increases, resulting in an enhancement in the removal of BB9. Also lower adsorption of BB9 at acidic pH is due to the presence of excess H^+ ions competing with the dye cation for the adsorption. For this reason basic pH (10–12) was selected for subsequent experimental work. Similar trend was observed by other workers for the adsorption of basic dye on bagasse ash (Mall et al., 2005).

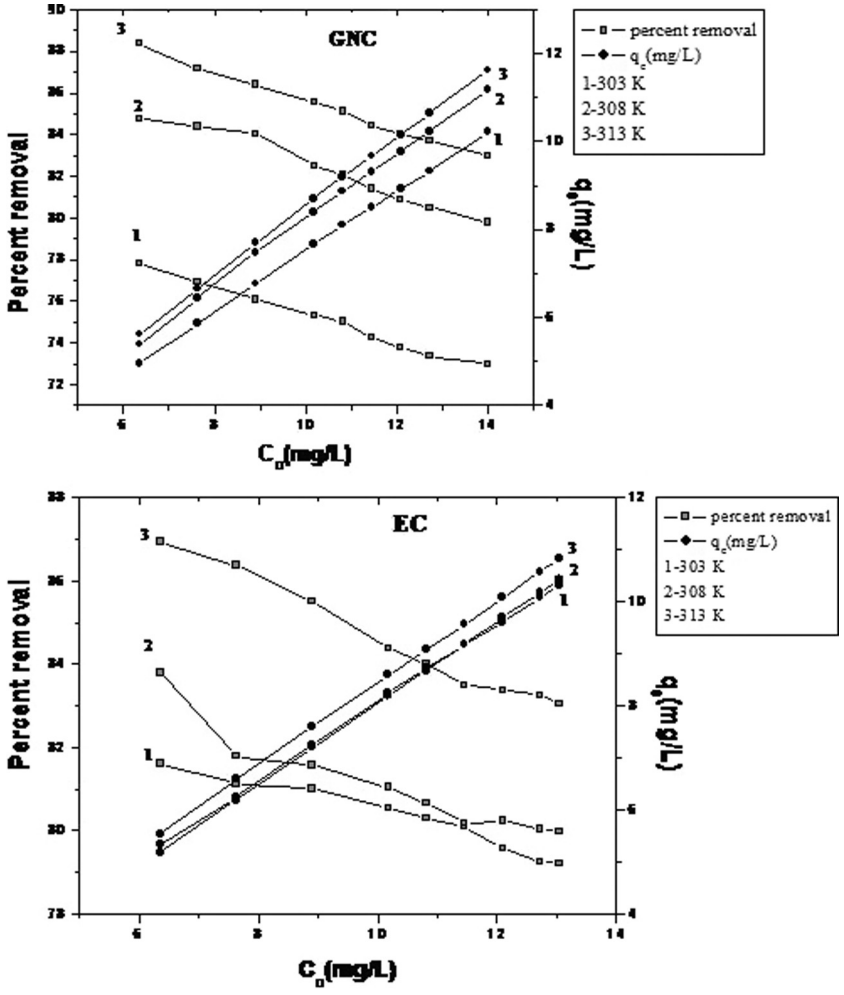

Figure 8 Effect of initial concentration of dye BB9 on GNC and EC. Adsorbent dosage = 1 g/L (□-% color removal, •-q_e (mg/g)).

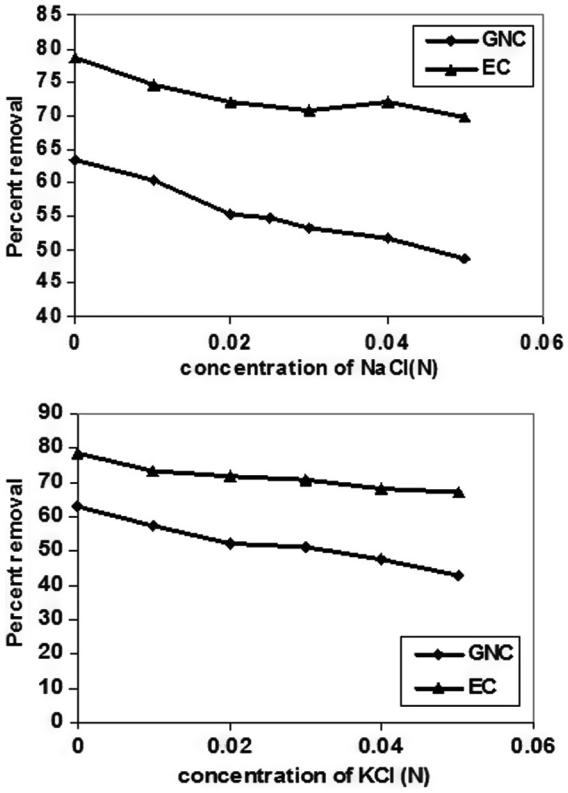

Figure 9 Effect. of ionic strength on adsorption of BB9 on GNC and EC. 1 – NaCl, 2 – KCl (Co = 14 mg/L, adsorbent dosage = 1 g/L).

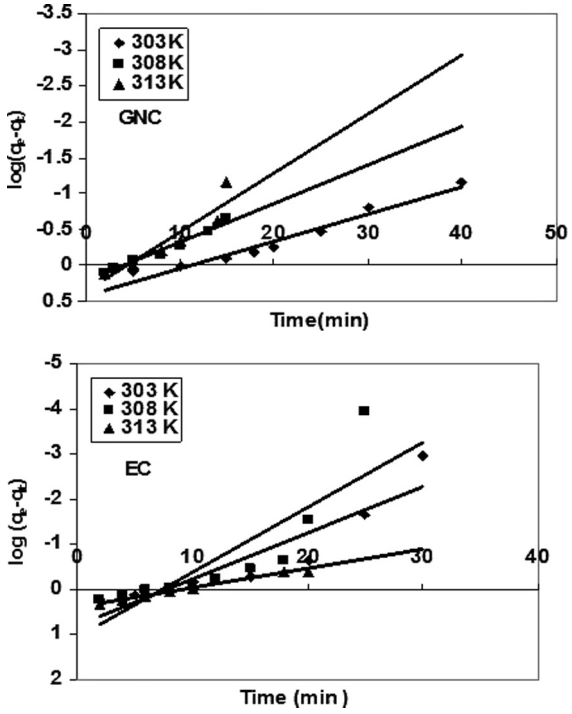

Figure 10 Pseudo-first-order kinetic plots for the removal of BB9 on GNC and EC (Co = 14, mg/L, adsorbent dosage = 1 g/L).

In order to confirm these results, the pH of point of zero charge (pH_{pzc}) of samples was carried out by the procedure described by Rivera-Utrilla et al. (2001). The pH_{pzc} is defined by the point where the curve $pH_{initial}$ vs pH_{final} crosses the line $pH_{initial} = pH_{final}$. The pH_{pzc} was determined and the values obtained for GNC and EC were at pH 9.1 and pH 7.8 respectively. The pH above pH_{pzc}, the surface of the adsorbent is negative and there is strong electrostatic attraction between the surface group and the dye BB9 (Saka and Sahin, 2011).

3.8. Effect of initial concentration

A study of the effect of change in the amount adsorbed with initial concentration of the dye was carried out. From the Fig. 8 it is evident that BB9 percentage removal decreases with increase in Co, but the actual amount of the dye adsorbed for both the adsorbents increased with increase in adsorbate concentration. It is due to decrease in the resistance to the uptake of BB9 from the solution which increases the diffusion of the dye.

3.9. Effect of ionic strength

In dye processing, NaCl, KCl and Na_2SO_4 salts are used to enhance the bath exhaustion (Karadag et al., 2007). Different concentrations of NaCl and KCl (0.01–0.05 N) were added to the aqueous solutions of dye to investigate the effect of ionic strength on dye adsorption. Fig. 9 shows that increase in ionic strength causes decrease in adsorption of dye BB9 on both the adsorbents. In the literature, same effect has been reported for some cationic dyes (Karadag et al., 2007). It has been reported that an increase in ionic strength leads to decrease of the thickness of the electrical double layer and finally decreases the adsorption capacity of cationic dyes.

3.10. Adsorption kinetic study

3.10.1. Pseudo first order and pseudo second order models

The pseudo-first-order equation is given as (Lagergren, 1898).

$$\frac{dq_t}{dt} = k_f(q_e - q_t) \quad (1)$$

where q_t is the amount of dye adsorbed at time t (mg/g). q_e is the adsorption capacity at equilibrium(mg/g), k_f (min^{-1}) is the pseudo first orders rate constant, and t is the contact time (min). The integration of Eq. (1) with initial condition ($q_t = 0$ at $t = 0$) leads to following equation:

$$\log(q_e - q_t) = \log q_e - \frac{k_f}{2.303}t \quad (2)$$

The values of k_f for the adsorption of dye BB9 on GNC and EC which are determined by the linear plot of $\log(q_e - q_t)$ vs t are given in Table 1, Fig. 10.

The pseudo-second-order model is represented as (Ho and Mckay 2000).

$$\frac{dq_t}{dt} = k_s(q_e - q_t)^2 \quad (3)$$

where k_s is the pseudo second order rate constant (g mg^{-1} min^{-1}). Integrating Eq. (3) ($q_t = 0$ at $t = 0$) gives:

$$\frac{t}{q_t} = \frac{1}{k_s q_e^2} + \frac{1}{q_e}t \quad (4)$$

Table 1 Kinetic parameters for removal of BB9 on GNC and EC.

Equations	Parameters	Adsorbents					
		GNC			EC		
		303 K	308 K	313 K	303 K	308 K	313 K
Pseudo first order	q_e exp (mg/g)	10.13	11.52	11.58	11.20	11.31	11.72
	q_e cal (mg/g)	2.57	1.65	1.47	4.28	11.32	11.57
	k_f (min^{-1})	0.09	0.12	0.08	0.20	0.33	0.46
	R^2	0.97	0.98	0.98	0.96	0.90	0.92
Pseudo-second-order	q_e exp (mg/g)	10.13	11.52	11.58	11.20	11.31	11.72
	q_e cal (mg/g)	10.44	11.32	11.58	11.43	11.58	12.12
	k_s (g/mg min)	0.066	0.180	0.188	0.123	0.116	0.127
	R^2	0.99	0.99	0.99	0.99	0.99	0.99
Intra-particle diffusion	k_{id} (mg/g $min^{1/2}$)	0.29	0.39	0.48	0.43	0.47	0.64
	C (mg/g)	8.23	9.76	9.39	9.04	9.08	9.18
	R^2	0.98	0.99	0.98	0.97	0.99	0.98
Bangham	k_o (g)	58.93	73.77	71.16	108.9	104.4	102.4
	α	0.064	0.040	0.060	0.176	0.138	0.133
	R^2	0.97	0.98	0.98	0.98	0.98	0.98
Elovich	a	2.3×10^5	8.5×10^7	3.5×10^6	7.2×10^5	4.5×10^5	0.6×10^5
	b	1.65	1.94	1.63	1.54	1.47	1.20
	R^2	0.97	0.98	0.98	0.98	0.98	0.98

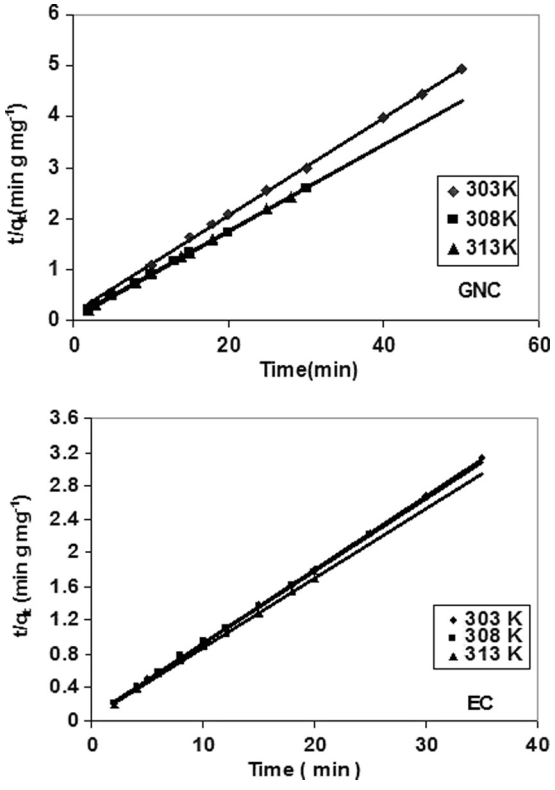

Figure 11 Pseudo-second order kinetic plots for the removal of BB9 on GNC and EC (Co = 14, mg/L, adsorbent dosage = 1 g/L).

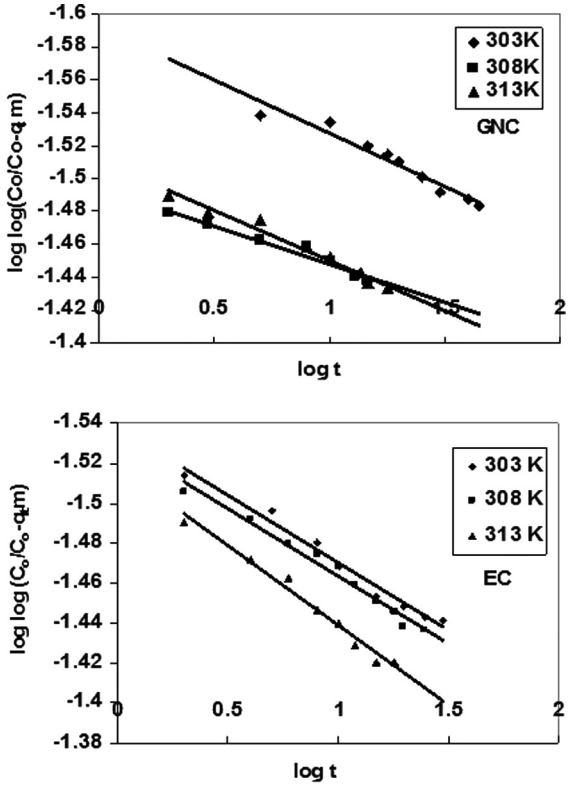

Figure 12 Bangham's plots for the removal of BB9 on GNC and EC (Co = 14 mg/L, adsorbent, dosage = 1 g/L).

Fig. 11 shows the plot of t/q_t versus t. The equilibrium adsorption capacity, q_e is obtained from the slope and k_s is obtained from the intercept. The values are given in Table 1. The q_e experimental and the q_e calculated values from the pseudo second-order kinetic model are very close to each other. The calculated correlation coefficients ($R^2 = 0.99$) are also close to unity for pseudo-second order kinetic than that for the pseudo-first order kinetic model. Therefore, the sorption can be approximated more appropriately by pseudo second order kinetic model than the first-order kinetic model for both the studied adsorbents.

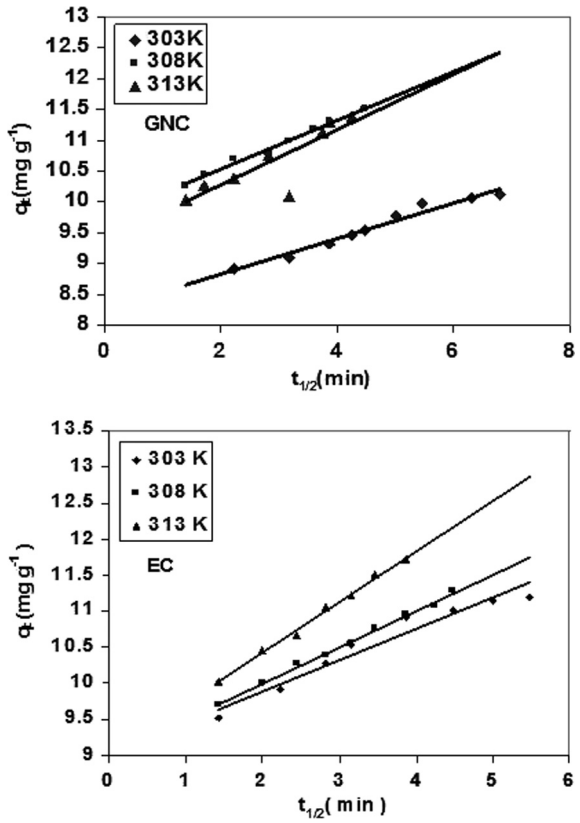

Figure 13 Weber and Morris intra-particle diffusion plots for the adsorption of BB9 on GNC, and EC (Co = 14 mg/L, adsorbent dosage = 1 g/L).

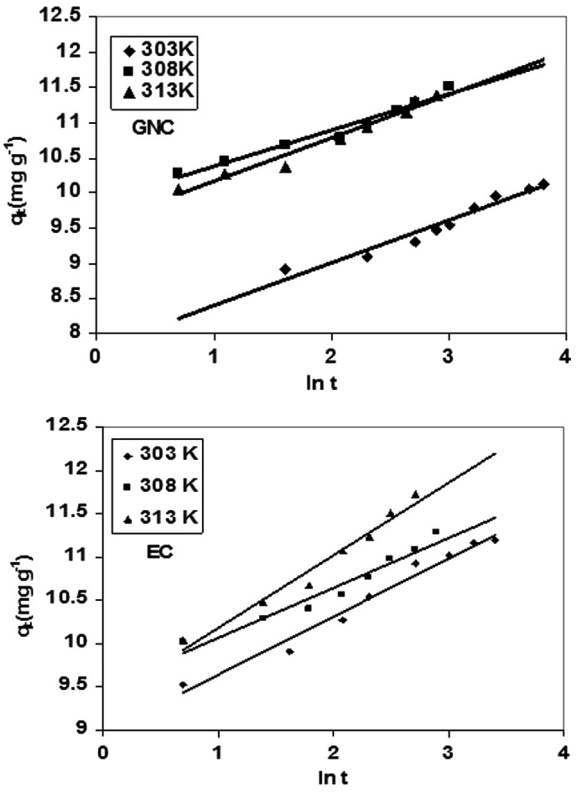

Figure 14 Elovich kinetic plots for the removal of BB9 on GNC and EC (Co = 14 mg/L, adsorbent dosage = 1 g/L).

3.10.2. Bangham's equation

Kinetic data were further used to know about the slow step occurring in the present adsorption system using Bangham's equation (Tutem et al., 1998).

$$\mathrm{Log}(C_o/C_o - q_t m) = log(k_o m/2.303V) + \alpha \log t \quad (5)$$

where C_o is the initial concentration of dye in solution (mg/L), V is the volume of the solution (mL), m is the weight of adsorbent per liter of solution (g/L), q_t (mg/g) is the amount of dye adsorbed at time t and $\alpha(<1)$ and k_o are constants. The double logarithmic plots are shown in Fig. 12. Linear plot shows that the diffusion of adsorbate into the pores of adsorbents is not the only rate controlling step (Tutem et al., 1998)

3.10.3. Intra-particle diffusion study

An empirically found functional relationship common to most adsorption process, is that the uptake varies almost proportionally with $t_{½}$, the Weber–Morris plot, rather than with the contact time, t (Weber and Morris, 1963).

$$q_t = k_{id} t_{1/2} + C \quad (6)$$

where k_{id} is the intra-particle diffusion rate constant. According to Eq. (6), a plot of q_t versus $t_{½}$ should be a straight line with a slope k_{id} and intercept C when adsorption mechanism follows the intra-particle diffusion process. Values of the intercept gives an idea about the thickness of boundary layer i.e. larger the intercept the greater is the boundary layer effect (Kannan and Sundaram, 2001). Plot of q_t vs $t_{1/2}$ is illustrated in Fig. 13. The linearity is attributed to the macropore diffusion, which is an accessible site of adsorption. This is attributed to the instantaneous utilization of the most readily available adsorbing sites on the adsorbent surface .The values of k_{id} obtained from the slope of plots are listed in Table 1.

3.10.4. Elovich model

The Elovich equation generally used is expressed as (Wang et al., 2009).

$$q_t = \frac{1}{b}\ln(ab) + \frac{1}{b}\ln t \quad (7)$$

where q_t (mg/g) is the amount of dye adsorbed at time t (min) and a and b are the constants. The chemical significance of these constants has not been clearly resolved (Wang et al., 2009). Fig. 14, shows the plot q_t versus ln t having slope 1/b and intercept [(1/b) ln(ab)].The values of a and b are given in Table 1.

3.11. Adsorption Isotherms

Various isotherm equations have been used to describe the equilibrium nature of adsorption.

3.11.1. Langmuir isotherm

The linear form of Langmuir Isotherm is represented by the following equation.

$$C_e/q_e = C_e/C_m + 1K_L C_m \quad (8)$$

where C_e is the concentration of dye solution (mg/L) at equilibrium. The constant C_m signifies the adsorption capacity

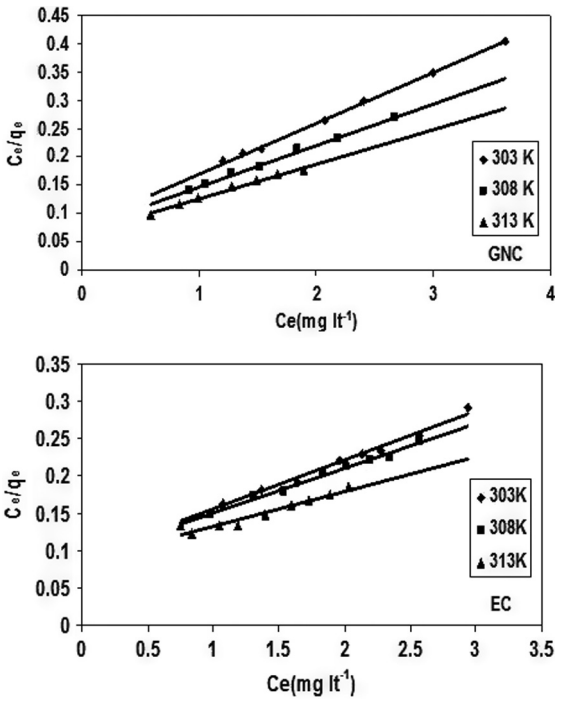

Figure 15 Langmuir isotherm plots for the removal of BB9 on GNC and EC (Co = 14 mg/L, adsorbent dosage = 1 g/L).

(mg/g) and K_L (L/mg) is related to the energy of adsorption. Langmuir plot is shown in Fig. 15. The values of K_L and C_m (monolayer concentration) were calculated from the intercept and slope of the plots are given in Table 2. Maximum adsorption capacity increased with an increase in the temperature revealing the endothermic nature of the adsorption process. In the present work the maximum adsorption capacity was found to be 16.4 and 21.8 mg/g for GNC and EC respectively for the studied dye BB9. However activated clay shows the capacity of 57.8 mg/g for acid blue 9 (Gupta and Suhas, 2009) and mixture of activated clay and chitosan enhances the adsorption capacity to 330 mg/g for the dye BB9 (Wan Ngah et al., 2011).

To identify the feasibility and favorability of the adsorption process, an approach recommended by Weber and Chakrabarti (Weber and Chakrabarti, 1974) was adopted as dimensionless constant, separation factor (R_L) (Hall et al., 1966) was calculated in each case using the following equation:

$$R_L = 1/(1 + K_L C_o) \quad (9)$$

where C_o is the initial dye concentration (mg/L). The values of 'R_L' were found to be less than unity for both the studied adsorbents (Table 3) and imply highly favorable adsorption for the dye BB9.

3.11.2. Freundlich isotherm

This isotherm is an empirical equation employed to describe the heterogeneous system (Crini and Peindy, 2006). Freundlich isotherm is also applied to plot the equilibrium data of the adsorption.

$$\log x/m = \log K_F + 1/n \log C_e \quad (10)$$

where x is the amount of dye adsorbed (mg), m is the weight of the adsorbent used (g), C_e is the equilibrium concentration of the dye in solution (mg/L) and K_F and n are Freundlich constants, n is heterogeneity factor (adsorption intensity) and K_F denotes the adsorption capacity. The values of $n > 1$, reflecting the favorable adsorption conditions (Crini and Peindy, 2006). Freundlich plots are shown in Fig. 16 and linearity suggests that fit is well for the adsorption system under the studied concentration range. The values of n and K_F are calculated from the slopes and intercepts of the linear plots are recorded in Table 2. Increase in adsorption capacity (K_F) with temperature substantiated the endothermic adsorption.

3.11.3. Dubinin and Radushkevich (D–R) isotherm

This isotherm expressed as follows (Dubinin, 1960):

$$q_e = q_s \exp(-B\epsilon^2) \quad (11)$$

where q_s is D–R constant and ϵ can be correlated as

$$\epsilon = RT \ln(1 + 1/C_e) \quad (12)$$

Table 2 Isotherms parameters for removal of BB9 on GNC and EC.

Equations	Parameters	Adsorbents					
		GNC			EC		
		303 K	308 K	313 K	303 K	308 K	313 K
Freundlich	K_F (mg/g)(L/mg)$^{1/n}$	6.09	6.85	7.74	6.56	6.75	7.42
	N	3.21	2.56	2.04	2.22	2.06	2.06
	R^2	0.98	0.98	0.99	0.97	0.99	0.99
Langmuir	K_L (L/mg)	1.06	1.02	0.93	0.73	0.66	0.53
	C_m (mg/g)	11.29	13.45	16.36	15.21	16.79	21.76
	R^2	0.99	0.98	0.98	0.99	0.99	0.96
Dubinin Radushkevih	q_s (mg/g)	9.38	10.55	11.36	11.39	11.66	13.19
	E (kJ/mol)	1.69	1.88	2.21	1.56	1.65	1.73
	R^2	0.97	0.98	0.98	0.99	0.98	0.99
Temkin	K_T (L/mg)	12.67	8.60	7.38	5.56	5.03	4.37
	B_1	2.35	3.17	3.94	3.75	4.11	5.14
	R^2	0.98	0.97	0.99	0.98	0.99	0.98
Generalized	N	0.99	0.97	0.99	1.01	0.99	0.89
	K_G (mg/L)	6.20	3.01	1.03	1.37	1.52	1.79
	R^2	0.99	0.99	0.99	0.98	0.99	0.99

Table 3 Values of R_L and thermodynamic parameters for the adsorption of BB9.

Adsorbents	Temp. (K)	R_L values	$-\Delta G$ (kJ mol^{-1})	ΔH (kJ mol^{-1})	ΔS (JK^{-1} mol^{-1})	R^2
GNC	303	0.063	32.06	10.29	71.97	0.97
	308	0.065	32.49			
	313	0.071	32.79			
EC	303	0.089	31.14	25.19	19.78	0.97
	308	0.097	31.94			
	313	0.112	31.33			

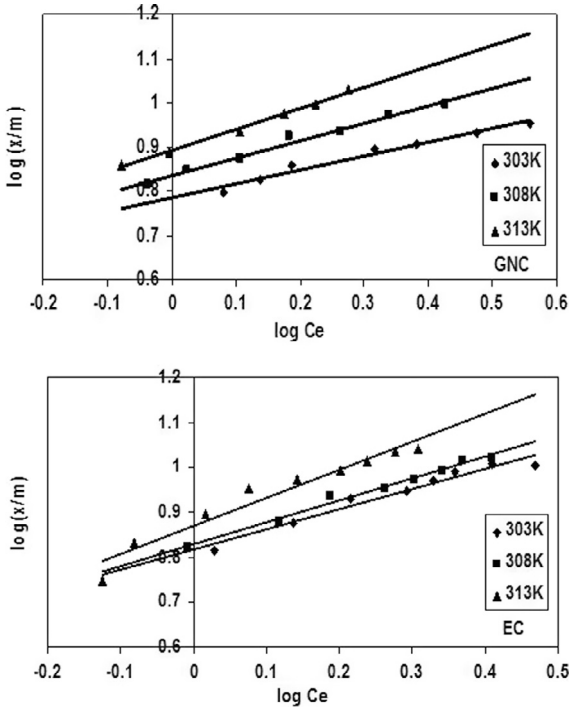

Figure 16 Freundlich isotherm plots for the removal of BB9 on GNC and EC (Co = 14 mg/L, adsorbent dosage = 1 g/L).

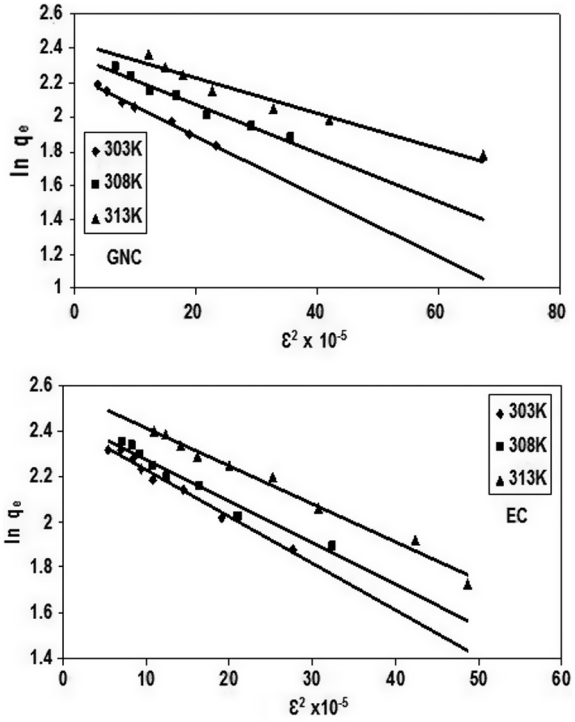

Figure 17 D-R isotherm plots for the removal of BB9 on GNC and EC (Co = 14 mg/L, adsorbent dosage = 1 g/L).

The constant B gives the mean free energy E of the adsorption per molecule of adsorbate when it is transferred into the surface of the solid from infinity in the solution and can be calculated using the following equation:

$$E = 1/(2B)^{1/2} \quad (13)$$

The D–R isotherm plotted against experimental values is shown in Fig. 17. The calculated D–R constant is given in Table 2. It is clear that adsorption energy value increased with increase in the temperature for the adsorption of BB9 on GNC and EC intimating endothermic behavior.

3.11.4. Temkin isotherm

The Temkin isotherm equation assumes that the fall in the heat of adsorption of all the molecules in the layer decreases linearly with coverage due to adsorbent–adsorbate interactions, and that the adsorption is characterized by a uniform distribution of the binding energies up to some maximum binding energy (Aharoni and Ungarish, 1977). The Temkin isotherm has been applied in the following form.

$$q_e = B_1 \ln K_T + B_1 \ln C)e \quad (14)$$

where $B_1 = RT/b$.

A plot of q_e verses ln C_e enables the determination of the isotherm constant K_T and B_1. K_T is the equilibrium binding constant (L/mg) corresponding to the maximum binding energy and constant B_1 is related to the heat of adsorption. The Temkin isotherm plotted against the experimental values are shown in Fig. 18 and the values of the constants are given in Table 2.

3.11.5. Generalized isotherm

The generalized isotherm is given as (Kargi and Ozminci, 2004).

$$\ln[(q_{max}/q_e) - 1] = \ln K_G - N \ln C_e \quad (15)$$

where K_G is the saturation constant (mg/L), N is the cooperative binding constant, q_{max} is the maximum adsorption capacity of the adsorbent (mg/g). q_e (mg/g) and C_e (mg/L) are the equilibrium dye concentrations in the solid and liquid phase, respectively. A plot of $\ln[q_{max}/q_e - 1]$ verses ln C_e is shown in Fig. 19. The values of K_G and N are calculated from the slope and intercept of the plot and these values are given in Table 2.

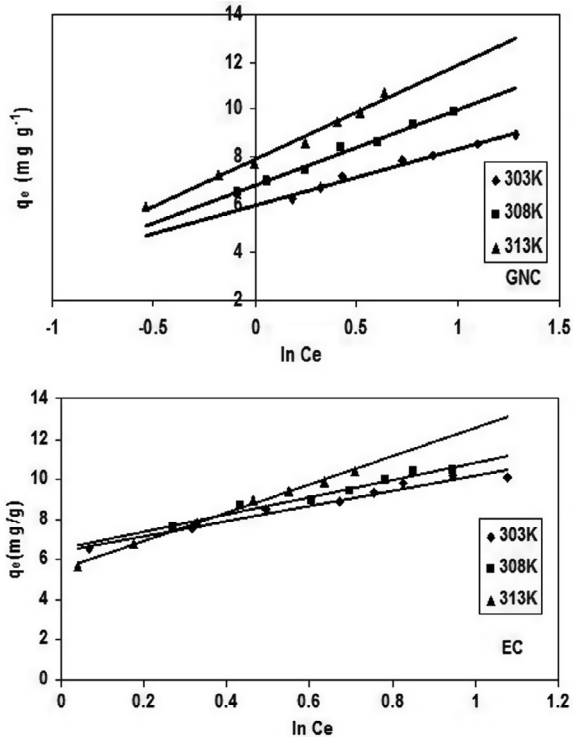

Figure 18 Temkin isotherm plots for the removal of BB9 on GNC and EC (Co = 14 mg/L, adsorbent dosage = 1 g/L).

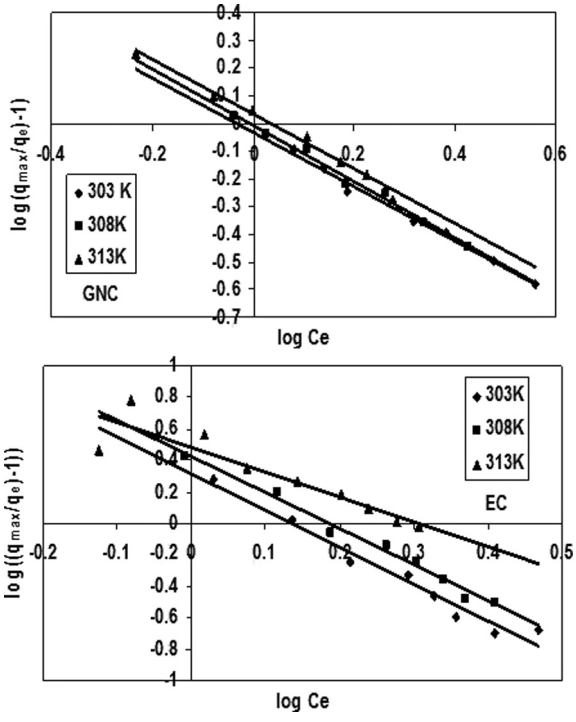

Figure 19 Generalized isotherm plots for the removal of BB9 on GNC and EC (Co = 14 mg/L, adsorbent dosage = 1 g/L).

3.12. Thermodynamic parameters

Thermodynamic parameters (changes in standard Gibb's free energy ΔG, enthalpy change ΔH, and entropy change ΔS) were calculated using the following equations:

$$\Delta G = -\mathrm{RT}\ln K_{\mathrm{L}} \tag{16}$$

$$\Delta G = \Delta H - T\Delta S \tag{17}$$

where K_{L} is Langmuir constant when concentration terms are expressed in L/mol. The plot of ΔG versus T was found to be linear and ΔH and ΔS values were calculated from the intercept and slope of the plot by linear regression method are listed in Table 3. The positive values of ΔH confirmed the endothermic nature of adsorption process, and positive value of ΔS revealed the increase in randomness at the solid/solution interface during the adsorption process. The negative ΔG value indicates the feasibility of the adsorption process. Similar results were reported by Zhang et al. for the removal of malachite green from aqueous solutions (Zhang et al., 2008).

4. Conclusion

- Adsorption of dye BB9 increased with contact time, temperature, adsorbent dose and initial concentration (Co), however it decreases with increase in ionic strength.
- Equilibrium time decreases with increase in temperature established that adsorption of BB9 is favored at high temperature and signifies the endothermic nature of adsorption of BB9 on GNC and EC.
- The values of $R_{\mathrm{L}} < 1$ (Hall constant), obtained in this study indicate the applicability of Langmuir adsorption isotherm and highly favorable adsorption.
- Adsorption of BB9 on both the adsorbents is approximated more appropriately by pseudo second order kinetic model as is evidenced by q_{e} and R^2 values.
- Intraparticle diffusion constant (K_{id}), adsorption capacity (K_{F}) and monolayer concentration (C_{m}) increase with the increase in temperature revealed that adsorption of BB9 on GNC and EC is endothermic and it is further strengthened by the positive values of change in enthalpy.
- The spontaneity and feasibility of the adsorption process are shown by the negative values of ΔG.
- Hence charcoal prepared from waste materials, ground nut shells (GNC), and Eichhornia (EC) was found to be cost effective in removing BB9 dye from aqueous solutions. It is hoped that these studies can be extended further for the removal of colored effluents of dyeing and processing industries.

References

Aharoni, C., Ungarish, M., 1977. Kinetics of activated chemisorptions. Part 2. Theoretical models J. Chem. Soc. Faraday Trans. 73, 456–464.

Alpat, S.K., Alpat, O.O.S., Akay, H., 2008. The adsorption kinetic and removal of cationic dye, Toludine Blue O from aqueous solutions with turbish zeolite. J. Hazard. Mater. 15, 213–220.

Annadurai, G., Juang, R.S., Lee, D.L., 2002. Adsorption of heavy metals from water using banana and orange peels. Water Sci.Technol. 47, 185–190.

Barka, N., Qourzal, S., Assabbane, A., Nounah, A., Ait-Ichou, Y., 2010. Photocatalytic degradation of an azo reactive dye, Reactive Yellow 84, in water using an industrial titanium dioxide coated media. Arab. J. Chem. 3, 279–283.

Chan, L.S., Cheung, W.H., Mckay, G., 2008. Adsorption of acid dyes by bamboo derived activated carbon. Desalination 218, 304–312.

Chiou, M.S., LI, H.Y., 2002. Equilibrium and kinetic modelling of adsorption of reactive dye on cross linked chitosan beads, J. Hazard. Mater. 93, 233–248.

Coro, E., Laha, S., 2001. Color removal from Textile Effluents Using Hardwood as an Adsorbent. Water Res. 35 (7), 1851–1854.

Crini, G., 2008. Kinetic and equilibrium studies on removal of cationic dyes from aqueous solutions by adsorption onto a cyclodextrin polymer. Dyes Pigm.77, 415–426.

Crini, G., Peindy, H.N., 2006. Adsorption of C. I Basic Blue on cyclodextrin-based material containing carboxylic groups. Dyes Pigme. 70, 204–211.

Dizge, N., Aydiner, C., Demirbas, E., Kobya, M., Kara, S., 2008. Adsorption of reactive dyes from aqueous solutions by fly ash: Kinetic and equilibrium studies. J. Hazard. Mater. 150, 737–746.

Dogen, M., Alkan, M., 2003. Adsorption kinetic of methyl violet onto perlite. Chemosphere 50, 517–528.

Dubinin, M.M., 1960. The potential theory of adsorption of gases and vapors for adsorbents with energetically non-uniform surface. Chem. Rev. 60, 235–241.

Gong, R., Jin, Y., Chen, J., Hu, Y., Sun, J., 2007. Removal of basic dyes from aqueous solution by sorption on phosphoric acid modified rice straw. Dyes Pigm. 73, 332–337.

Gupta, V.K., Suhas, Ali, I., Saini, V.K., 2004. Removal of Rhodamine B, Fast Green and Methylene blue from wastewater using Red Mud, an Aluminum industry waste. Ind. Eng. Chem. Res. 43, 1740–1747.

Gupta, V.K., Suhas, 2009. Application of low cost adsorbents for dye removal – a review. J. Environ. Manag. 90, 2313–2342.

Hall, K.R., Eagleton, L.C., Acrivos, A., Vermenlem, T., 1966. Pore and solid diffusion kinetics in fixed adsorption constant pattern conditions. Ind. Eng. Chem. Funda. 5, 212–223.

Ho, Y.S., Mckay, G., 2000. The kinetic of the sorption of divalent metal ions on to sphagnum moss peat. Water Res. 34, 735–742.

Kannan, K., Sundaram, M.M., 2001. Kinetics and mechanism of removal of methylene blue by adsorption on various carbon – a comparative study. Dyes Pigm. 51, 25–40.

Karadag, D., Akgul, E., Tok, S., Erturk, F., Kaya, M.A., Turan, M., 2007. Basic and reactive dye removal using natural and modified zeolites. J. Chem. Eng. Data 52, 2436–2441.

Kargi, F., Ozminci, S., 2004. Biosorption performance of powdered activated sludge for removal of different dyestuff. Enzyme Microbial Tech. 35, 267–271.

Lachman, L., Lieberman, H.A., The theory and practice of industrial pharmacy, CBS publishers, special Indian Edition(2009) 27.

Lagergren, S., 1898. Zur theorie der sogenannten adsorption geloster stoffe kungliga Sevenska Vetenskapasakademiens. Handlingar 24, 1–39.

Lakshmi, U.R., Srivastava, V.C., Mall, I.D., Lataye, D.H., 2009. Rice husk ash as an effective adsorbent: Evaluation of adsorptive characteristics for Indigo Carmine Dye. J. Environ. Manag. 90, 710–720.

Leechart, P., Nakbanpote, W., Thiravetyan, P., 2009. Application of 'waste' wood-shaving bottom ash for adsorption of azo reactive dye. J. Environ. Manag. 90, 912–920.

Mall, I.D., Srivastava, V.C., Ararwal, N.K., Mishra, I.M., 2005. Adsorptive removal of malachite green dye from aqueous solution by baggase fly ash and activated carbon –kinetics study and equilibrium isotherm analyses. Colloids Surf. A Physicochem. Eng. Aspect 264, 17–28.

Mittal, A., Gajbe, V., Mittal, J., 2008. Removal and recovery of hazardous triphenylmethane dye, Methyl Violet through adsorption over granulated waste materials. J. Hazard. Mater. 150, 364–375.

Mohan, D., Singh, K.P., Singh, G., Kumar, K., 2002. Removal of dyes from wastewater using fly ash, a low-cost adsorbent. Ind. Eng. Chem. Res. 41, 3688–3695.

Namasivayam, C., Prabha, D., Kumutha, M., 1998. Removal of direct red and acid brilliant blue by adsorption onto banana pith. Bioresour. Technol. 64, 77–79.

Rivera-Utrilla, J., Bautista- Toledo, I., Ferro- Garcia, M.A., Moreno-Castilla, C., 2001. Activated carbon surface modifications by adsorption of bacteria and their effect on aqueous lead adsorption. J. Chem. Technol. Biotechnol. 76, 1209–1215.

Ruthven, D.M., 1984. Principles of Adsorption and Desorption Processes. John Wiley and Sons, New York.

Saka, C., Sahin, O., 2011. Removal of methylene blue from aqueous solutions by using cold plasma- and formaldehyde- treated onion skins. Color. Technol. 127, 246–255.

Salem, I.A., El-maazawi, M., 2000. Kinetics and Mechanism of color removal of Methylene blue with hydrogen peroxide catalysed by some supported alumina surfaces. Chemosphere 41, 1173–1180.

Stephenson, R.J., Sheldon, J.B., 1996. Coagulation and precipitation of a Mechanical Pupling Effluent: Removal of Carbon and Turbidity. Water Res. 30 (4), 781–792.

Sumanjit, Walia, T.P.S., 2008a. Use of dairy sludge for the removal of some basic dyes. J. Environ. Eng .Sci. 7, 433–438.

Sumanjit, Prasad, N., 2001. Adsorption of dyes on rice husk ash. Ind. J. Chem. 40A, 388–391.

Sumanjit, Walia, T.P.S., Mahajan, R.K., 2008b. Studies of zinc, cadmium, lead and copper on economically viable adsorbents. J. Environ. Eng. Sci. 7, 83–90.

Sun, Q., Yang, L., 2003. The adsorption of basic dyes from aqueous solution on modified peat-resin particle. Water Res. 37, 1535–1544.

Tutem, E., Apak, R., Unal, C.F., 1998. Adsorptive removal of chlorophenols from water by bituminous shale. Water Res. 32, 2315–2324.

Unuabonah, E.I., Adebowale, K.O., Dawodu, F.A., 2008. Equilibrium, kinetic and sorber design studies on the adsorption of Aniline blue by sodium tetraborate-modified Kaolinite clay adsorbent. J. Hazard. Mater. 157, 397–409.

Wan Ngah, W.S., Teong, L.C., Manafiah, M.A.K.M., 2011. Adsorption of dyes and heavy metal ions by chitosan composites: a review. Carbohydr. Polym. 83, 1446–1456.

Wang, S., Li, H., 2007. Kinetics modelling and mechanism of dye adsorption on unburned carbon. Dyes Pigm. 72, 308–314.

Wang, X.S., Li, Z.Z., Tao, S.R., 2009. Removal of chromium (VI) from aqueous solution using walnut hull. J. Environ. Manag. 90, 721–729.

Wang, X.S., Zhou, Y., Jiang, Y., Sun, C., 2008. The removal of basic dyes from aqueous solutions using agriculture by products. J. Hazard. Mater. 157, 374–385.

Weber Jr., W.J., Morris, J.C., 1963. Kinetics of adsorption on carbon from solution. J. Saint. Engg. Divi, American. Soc. Civil. Engg. 89, 31–59.

Weber, T.W., Chakrabarti, R.K., 1974. Pore and solid diffusion models for fixed bed adsorbers. J.Amer.Inst. Chem.Engg. 20, 228–238.

Wong, Y.C., Szeto, Y.S., Cheung, W.H., Mckay, G., 2004. Adsorption of acid dyes on chitosan-equilibrium isotherm analyses. Process Biochem. 39, 693–702.

Zhang, J., Li, Y., Zhang, C., Jing, Y., 2008. Adsorption of malachite green from aqueous solution onto carbon prepared from Arundo donax root. J. Hazard. Mater. 150, 774–782.